Advances in Aircraft and Spacecraft Science, *Vol. 11, No. 4 (2024) 299-312*
https://doi.org/10.12989/aas.2024.11.4.299

Employing an analytical method for post-buckling analysis of functionally graded beams

Mokhtar Bouazza*[1,2], Khaled Amara[3,4] and Mohamed Zidour[5,6]

[1]*Department of Civil Engineering, University Tahri Mohammed of Bechar, Bechar 08000, Algeria*
[2]*Laboratory of Materials and Hydrology (LMH), University of Sidi Bel Abbes, Sidi Bel Abbes 2200, Algeria*
[3]*Engineering and Sustainable Development Laboratory, University of Ain Temouchent, Ain Temouchent 46000, Algeria*
[4]*Department of Civil Engineering, University of Ain Temouchent, Ain Temouchent 46000, Algeria*
[5]*Laboratory of Geomatics and Sustainable Development, University of Tiaret, BP 78 Zaaroura, 14000 Tiaret, Algeria*
[6]*Department of Civil Engineering, University of Tiaret, BP 78 Zaaroura, 14000 Tiaret, Algeria*

(Received May 31, 2024, Revised December 15, 2024, Accepted December 16, 2024)

Abstract. In this work, it would be very interesting to study the post-buckling response of FG beams with relatively simple boundary conditions, i.e., simply supported. The material properties of the beams are considered to vary continuously in the thickness direction according to the power-law form. The formulations used are based on the classical beam theory (CBT), and two higher order theories, such as, the hyperbolic shear deformation theory of beams (HSDBT) and the Aydogdu shear deformation theory (ASDBT). On the one hand, in this context, we examine the effects of two parameters, such as the slenderness ratio and material variations presented by the power index on the critical buckling load via the two formulations of beam theories. The results in the tables can be useful and can be considered as a reference with which other researchers can verify the accuracy of their results.

Keywords: ASDBT; beams, functionally graded materials; HSDBT; postbuckling CBT

1. Introduction

Functionally graded materials (FGMs) are new types of materials which are developed to meet current requirements and achieve a characteristic performance with graded variable properties in one direction or more directions (Yang and Chen 2008). This continuity is highly interesting to avoid the disadvantages of composite materials such as the initiation and propagation of cracks due to large plastic deformation at the interfaces, the phenomenon of delamination due to large interlaminar stresses. Typically, FGMs are made of a mixture of different metals and a combination of ceramics.

Various models of beam theories have been developed to establish the appropriate analysis of the functionally graded (FG) beams. The classical beam theory known as Euler-Bernoulli beam theory is the simplest one and is applicable to slender FG beams only. For moderately deep FG beams, the CBT overestimates natural frequency and underestimates deflection due to neglecting

*Corresponding author, Professor, E-mail: bouazza_mokhtar@yahoo.fr, bouazza.mokhtar@univ-bechar.dz

http://www.techno-press.org/?journal=aas&subpage=7 ISSN: 2287-528X (Print), 2287-5271 (Online)

the transverse shear deformation effect (Simsek and Kocaturk 2009). The CBT has been employed to predict the effect of temperature on the beams behavior strengthened by bonded composite plates by Bouazza *et al.* (2019a). Chakraborty and Gopalakrishnan (2003) presented wave propagation analysis in beams made of FGM by via the spectral finite element approach. Sankar (2001) study an elasticity solution for bending behavior of functionally graded (FG) beams based on CBT. Young's modulus was assumed to vary as an exponential function, while Poisson's ratio was set to be constant. Zhong and Yu (2007) using the Airy stress function to provide an analytical solution for cantilever beams subjected to various types of mechanical loadings. Axial vibration analysis of exponential power and sigmoid and FG nanobeams based on exact solution was analyzed by Hosseini *et al.* (2020).

In addition, the works proposed by Arefi and Zenkour (2016, 2017a, b, c, d, e, 2018, 2019) are worthy of interest have addressed several mechanical problems, free vibration, stability, bending and dynamics of magneto-electro-structures elastic nanobeam, sandwich microbeam with two integrated piezomagnetic face-sheets and piezo-magnetic curved nanobeam via higher-order shear deformation theory and strain gradient theory. Other interesting results on the analysis of nanobeams are given in the articles of (Qing and Cai 2023, Arefi *et al.* 2015, 2018, 2019, 2021, Tang and Qing 2023).

Further, Soldatos and Timarci (1993) used a 'zig-zag' displacement model that enables having a continuous distribution of the interlaminar through-the-thickness stresses to formulate a general theory that unifies most of the variationally consistent classical and shear deformable cylindrical shell theories. Karama *et al.* (2003) proposed an exponential variation for the transverse strain in their analysis of the bending behavior of laminated beams. Since the first order shear deformation beam theory violates the zero shear stress conditions on the top and bottom surfaces of the beam, a shear correction factor is required to account for the discrepancy between the actual stress state and the assumed constant stress state (Ghasemi and Masood Mohandes 2016, Ebrahimi and Farazmandnia 2018). Additionally, many higher-order shear deformation models have been proposed for analysis of plate and beam by various author (Derbale *et al.* 2021, Ellali *et al.* 2018, 2022, 2023, 2024a, b, c, d, e, Amara *et al.* 2016, Chaudhari *et al.* 2017, Nguyen and Tran 2018, Xu *et al.* 2018, Becheri *et al.* 2016, Tounsi *et al.* 2004, 2005, Boucheta *et al.* 2024). Wang and Yu (2014) developed a new variational asymptotic composite beam approach for thermoelastic analysis with various types of composite beams, including sandwich structure and laminates, under different boundary conditions. Moreover, recently, many new types of research have been carried out in the field of behavioral studies composite structures (Bouazza *et al.* 2013, 2017, 2019b, 2021, Houari *et al.* 2024, Osman *et al.* 2024, Atmane *et al.* 2016, Kenouza *et al.* 2024).

In this study, post-buckling analysis of functionally graded beams having simply supported boundary conditions is analyzed within the framework of the classical, hyperbolic shear deformation beam theory and an Aydogdu shear deformation beam theory. Analytical solutions are presented for simply-supported boundary conditions. The material properties of the FGM beams are assumed to vary according to a power-law distribution of the volume fraction of the constituents. Numerical examples are presented to show the influence of power law index and slenderness ratio effect on critical buckling loads.

2. Analysis

2.1 Material properties

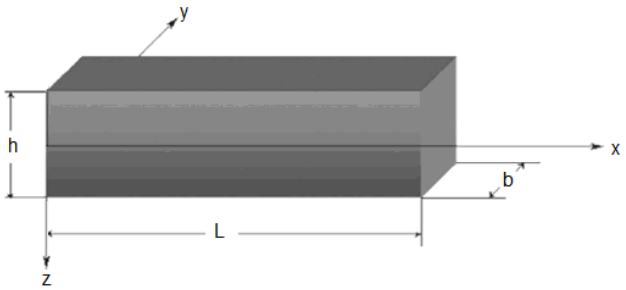

Fig. 1 Co-ordinates and geometry of FG beam

Consider a rectangular beam made of a mixture of metal and ceramic as shown in Fig. 1. The material in top surface and in bottom surface is metal and ceramic respectively. The modulus of elasticity, and the Poisson's ratio ν are assumed as (Yang and Chen 2008, Chakraborty and Gopalakrishnan 2003, Sankar 2001, Zhong and Yu 2007)

$$E(z) = E_c\ V_c\ + E_m\left(1 - V_c\ \right)$$
$$\nu(z) = \nu_0 \tag{1}$$

where E_c and E_m denote values of the elasticity modulus at the top and bottom of the beam, respectively, and k is a variable parameter. According to this distribution, bottom surface (*z*=-*h*/2) of functionally graded beam is pure metal, whereas the top surface (*z*=*h*/2) is pure ceramics, and for different values of k one can obtain different volume fractions of ceramic. V_c denotes the volume fraction of the ceramic and is assumed as a power function as follows

$$V_c\ = \left(\frac{z}{h} + \frac{1}{2}\right)^k \tag{2}$$

Fig. 2 shows the variation of volume fractions of ceramic in the thickness direction of FG beam. Here, volume fraction for ceramic increases from 0 at *z*=-*h*/2 to 1 at *z*=*h*/2. The state of stress in the beam is given by the generalized Hooke's law as follows

$$\sigma_x\ = Q_{11}\varepsilon_x\ \ ,\ \tau_{xz} = Q_{55}\gamma_{xz} \tag{3}$$

where Q_{ij} are the transformed stiffness constants in the beam co-ordinate system and are defined as

$$Q_{11} = \frac{E(z)}{1-\nu^2},\quad Q_{55} = \frac{E(z)}{2(1+\nu)} \tag{4}$$

2.2 Theory and formulations

High-order beam shear deformation theories have been developed in recent years, first for the analysis of several problems and then deployed to understand the physical phenomena induced in the beam. Unlike CBT and Timoshenko beam theory (TBT) with the assumptions of linear distribution of displacement through the thickness, HSDBT and ASDBT are based on a nonlinear distribution of fields in the section. Therefore, the effect of transverse shear deformation is taken into account. Based on the higher-order shear deformation theory, the axial displacement, U and

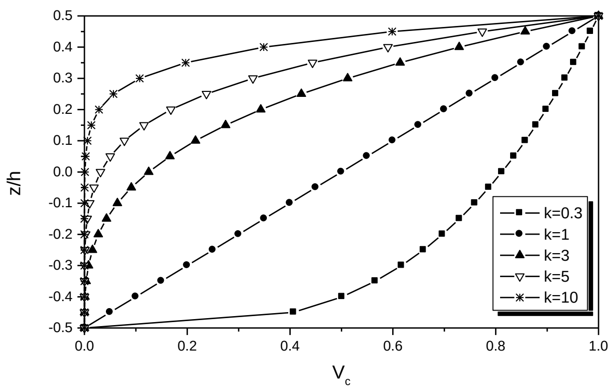

Fig. 2 Volume fraction of ceramic along the thickness direction the beam

the transverse displacement of any point of the beam, W, are given as (Simsek and Kocaturk 2009, Soldatos and Timarci 1993, Karama *et al.* 2003)

$$\begin{gathered} U(x,z,t) = u(x,t) - z\frac{\partial w}{\partial x}(x,t) + f(z)u_1(x,t) \\ W(x,z,t) = w(x,t) \end{gathered} \tag{5}$$

Here, u and w represent middle surface displacement components along the x and z directions, respectively, while u_1 is an unknown function that represents the effect of transverse shear strain on the beam middle surface, and $f(z)$ represents the shape function determining the distribution of the transverse shear strain and stress through the thickness. This is achieved by choosing the shape functions as follows

$$\begin{gathered} f(z) = 0 \\ f(z) = h\sinh\left(\frac{z}{h}\right) - z\cosh\left(\frac{1}{2}\right) \\ f(z) = z\alpha^{-2(z/h)^2/\ln\alpha} \text{ with } \alpha = 3 \end{gathered} \tag{6}$$

The nonvanishing strains related to the displacement field are obtained according to the two moderate-rotation and small-strain approximations, defined as follows

$$\begin{gathered} \varepsilon_x = \frac{\partial u}{\partial x} + \frac{1}{2}\left(\frac{\partial w}{\partial x}\right)^2 \\ \gamma_{xz} = \frac{\partial u}{\partial z} + \frac{\partial w}{\partial x} \end{gathered} \tag{7}$$

where ε_x is the normal deformation and γ_{xz} is the shear-deformation.

The axial displacement u is assumed to be of order 2, which is based on the assumption of the insignificant effect of the in-plane inertia. In this case from Eq. (5) and Eq. (7), we find the normal deformation and the shear-deformation

$$\varepsilon_x = \frac{\partial u}{\partial x} + \frac{1}{2}\left(\frac{\partial w}{\partial x}\right)^2 - z\frac{\partial^2 w}{\partial x^2} + f\frac{\partial u_1}{\partial x}$$

$$\gamma_{xz} = \frac{\partial f}{\partial x} u_1 \tag{8}$$

The stress results can be expressed as follows

$$N = \int_A \sigma_x dA, \quad M = \int_A z\sigma_x dA,$$
$$M^s = \int_A f\sigma_x dA, \quad Q^s = \int_A \frac{\partial f}{\partial x} \tau_{xw} dA, \tag{9}$$

where M^s and Q^s are stress resultants associated with the shear deformation, N and M are the classical well-known force and moment stress resultants, Using Hooke's law formula, the expression of stress-strains can be expressed as follows

$$\begin{Bmatrix} N \\ M \\ M^S \end{Bmatrix} = \begin{bmatrix} A_{11} & B_{11} & E_{11} \\ B_{11} & D_{11} & F_{11} \\ E_{11} & F_{11} & H_{11} \end{bmatrix} \begin{Bmatrix} \frac{\partial u}{\partial x} + \frac{1}{2}\left(\frac{\partial w}{\partial x}\right)^2 \\ -\frac{\partial^2 w}{\partial x^2} \\ \frac{\partial u_1}{\partial x} \end{Bmatrix} \tag{10a}$$

$$Q^s = A_{55} u_1 \tag{10b}$$

$$(A_{11}, B_{11}, D_{11}, E_{11}, F_{11}, H_{11}) = \int_A \left(1, z, z^2, f(z), zf(z), f(z)^2\right) Q_{11} dA, \tag{11}$$

Moreover, the transverse shear rigidity appearing in Eq. (10b) is defined according to

$$A_{55} = \int_A \left(\frac{\partial f}{\partial x}\right)^2 \bar{Q}_{55} dA \tag{12}$$

It should be pointed out that the extensional A_{11}, coupling B_{11} and bending D_{11} rigidities are the ones usually appearing even in the classical beam theories. Among the additional rigidities in Eq. (10a), the one denoted as E_{11} is considered as additional coupling rigidity while the ones denoted as F_{11} and H_{11} are considered as additional bending rigidities.

The governing stability equations of FG beam are given as follows (Nayfeh and Emam 2008)

$$\frac{dN}{dx} = 0 \tag{13}$$

$$\frac{dM^2}{dx^2} + \frac{d}{dx}\left(N\frac{dw}{dx}\right) - \bar{N}\frac{d^2 w}{dx^2} = 0 \tag{14}$$

$$\frac{dM^s}{dx} - Q^s = 0 \tag{15}$$

From Eqs. (13)-(15), the governing equations of the static response of the FG beam in terms of displacements can be given as follows

$$A_{11}\frac{\partial}{\partial x}\left(\frac{\partial u}{\partial x}+\frac{1}{2}\left(\frac{\partial w}{\partial x}\right)^2\right)-B_{11}\frac{\partial^3 w}{\partial x^3}+E_{11}\frac{\partial^2 u_1}{\partial x^2}=0 \tag{16}$$

$$A_{11}\frac{\partial}{\partial x}\left[\left(\frac{\partial u}{\partial x}+\frac{1}{2}\left(\frac{\partial w}{\partial x}\right)^2\right)\frac{\partial w}{\partial x}\right]+E_{11}\frac{\partial}{\partial x}\left(\frac{\partial w}{\partial x}\frac{\partial u_1}{\partial x}\right)+B_{11}\frac{\partial^3 u}{\partial x^3}$$
$$+F_{11}\frac{\partial^3 u_1}{\partial x^3}-D_{11}\frac{\partial^4 w}{\partial x^4}-\bar{N}\frac{\partial^2 w}{\partial x^2}=0 \tag{17}$$

$$E_{11}\frac{\partial}{\partial x}\left(\frac{\partial u}{\partial x}+\frac{1}{2}\left(\frac{\partial w}{\partial x}\right)^2\right)-F_{11}\frac{\partial^3 w}{\partial x^3}+H_{11}\frac{\partial^2 u_1}{\partial x^2}-A_{55}\frac{\partial u_1}{\partial x}=0 \tag{18}$$

We eliminate Eqs. (17) and (18) since Eq. (16) can be solved for the axial displacement *u* to lead to a model in terms of only the unknown displacements *w*, i.e., bending model. Using the expressions in Eq. (16) and integrating with respect to the spatial coordinate *x* gives

$$A_{11}\left(\frac{\partial u}{\partial x}+\frac{1}{2}\left(\frac{\partial w}{\partial x}\right)^2\right)-B_{11}\left(\frac{\partial w}{\partial x}\right)^2+E_{11}\frac{\partial u_1}{\partial x}=c_1 \tag{19}$$

where c_1 is a constant value that represents the tension force in the axial direction of the beam due to the stretching of the midplane. Integrating Eq. (19) again can be stated as

$$u(x)=-\frac{1}{2}\int_0^x\left(\frac{\partial w}{\partial x}\right)^2 d\xi+\frac{B_{11}}{A_{11}}\frac{\partial w}{\partial x}-\frac{E_{11}}{A_{11}}u_1+\frac{c_1}{A_{11}}x+c_2 \tag{20}$$

For the midplane stretching to be significant, the beam ends must be restrained. Kinematic boundary conditions for axial displacement are given as follows:

u=0 at x=0; L

This allows us to calculate the two coefficients c_1 and c_2 as follows

$$c_2=\frac{1}{A_{11}}\left[E_{11}u_1(0)-B_{11}\left.\frac{\partial w}{\partial x}\right|_{x=0}\right]$$
$$c_1=\frac{A_{11}}{2L}\int_0^L\left(\frac{\partial w}{\partial x}\right)^2 dx+\frac{E_{11}}{L}[u_1(L)-u_1(0)]-\frac{B_{11}}{L}\left[\left.\frac{\partial w}{\partial x}\right|_{x=L}-\left.\frac{\partial w}{\partial x}\right|_{x=0}\right] \tag{21}$$

When applying kinematic boundary conditions for displacement, Eq. (19) is rewritten as follows

$$\frac{\partial u}{\partial x}+\frac{1}{2}\left(\frac{\partial w}{\partial x}\right)^2=\frac{1}{2L}\int_0^L\left(\frac{\partial w}{\partial x}\right)^2 dx-\frac{E_{11}}{A_{11}}\frac{\partial u_1}{\partial x}+\frac{B_{11}}{A_{11}}\frac{\partial w}{\partial x}$$

$$+\frac{E_{11}}{LA_{11}}\left[\frac{\partial u_1}{\partial x}\bigg|_{x=L}-\frac{\partial u_1}{\partial x}\bigg|_{x=0}\right]-\frac{B_{11}}{LA_{11}}\left[\frac{\partial w}{\partial x}\bigg|_{x=L}-\frac{\partial w}{\partial x}\bigg|_{x=0}\right] \quad (22)$$

Eq. (16) can be derived as follows for simplicity

$$\frac{\partial}{\partial x}\left(\frac{\partial u}{\partial x}+\frac{1}{2}\left(\frac{\partial w}{\partial x}\right)^2\right)=-\frac{E_{11}}{A_{11}}\frac{\partial^2 u_1}{\partial x^2}+\frac{B_{11}}{A_{11}}\frac{\partial^3 w}{\partial x^3} \quad (23)$$

and

$$\frac{\partial^3 u}{\partial x^3}=-\frac{\partial}{\partial x}\left(\frac{\partial w}{\partial x}\frac{\partial^2 w}{\partial x^2}\right)-\frac{E_{11}}{A_{11}}\frac{\partial^3 u_1}{\partial x^3}+\frac{B_{11}}{A_{11}}\frac{\partial^4 w}{\partial x^4} \quad (24)$$

Substituting Eqs. (22)-(24) into Eqs. (17) and (18), we obtain

$$\left(\frac{B_{11}^2}{A_{11}}-D_{11}\right)\frac{\partial^4 w}{\partial x^4}-\left(\bar{N}-\frac{A_{11}}{2L}\int_0^L\left(\frac{\partial w}{\partial x}\right)^2 dx\right)\frac{\partial^2 w}{\partial x^2}+\left(F_{11}-\frac{B_{11}E_{11}}{A_{11}}\right)\frac{\partial^3 u_1}{\partial x^3}+\beta\frac{\partial^2 w}{\partial x^2}=0 \quad (25)$$

$$\left(H_{11}-\frac{E_{11}^2}{A_{11}}\right)\frac{\partial^2 u_1}{\partial x^2}+\left(\frac{B_{11}E_{11}}{A_{11}}-F_{11}\right)\frac{\partial^3 w}{\partial x^3}-A_{55}u_1=0 \quad (26)$$

Where β is a constant defined by

$$\beta=\frac{1}{L}\left\{E_{11}[u_1(L)-u_1(0)]-B_{11}\left[\frac{\partial w}{\partial x}\bigg|_{x=L}-\frac{\partial w}{\partial x}\bigg|_{x=0}\right]\right\} \quad (27)$$

In view of Eqs. (10a) and (10b), the stress resultants M and M^s are given by

$$M=-D_{11}\frac{\partial^2 w}{\partial x^2}+F_{11}\frac{\partial u_1}{\partial x}$$
$$M^s=-F_{11}\frac{\partial^2 w}{\partial x^2}+H_{11}\frac{\partial u_1}{\partial x} \quad (28)$$

Solving two equations for $\frac{\partial^2 w}{\partial x^2}$ and $\frac{\partial u_1}{\partial x}$ at the boundaries gives us

$$(F_{11}^2-H_{11}D_{11})\frac{\partial^2 w}{\partial x^2}(\xi)=0 \quad (29)$$

$$(F_{11}^2-H_{11}D_{11})\frac{\partial u_1}{\partial x}(\xi)=0, \text{ with } \xi=0, L \quad (30)$$

Because $F_{11}H_{11}$, and D_{11}, always different from zero, the two kinematic boundary conditions in terms of the displacement equation can be given as follows:

$$w=0 \text{ and } \frac{\partial u_1}{\partial x}=0 \text{ at } x=0, L$$

As is known, the only stable equilibrium position corresponds to the first buckling mode. For simply supported boundary conditions, Navier's method is used, and the displacements are expanded in trigonometric Fourier series in terms of unknown parameters. Therefore, the displacement field is written as follows

Table 1 Comparison of nondimensional first critical buckling load with different theories for several values of the material index, with *a*=0

L/h	Theory	*k*					
		*Fc**	0.3	1	3	5	*Fm***
5	HSDBT	4.410	3.447	2.611	1.997	1.741	0.812
	ASDBT	4.413	3.721	2.613	1.995	1.737	0.813
10	HSDBT	4.772	3.714	2.825	2.219	1.961	0.879
	ASDBT	4.773	3.788	2.826	2.218	1.960	0.879
20	HSDBT	4.872	3.787	2.885	2.283	2.025	0.897
	ASDBT	4.872	3.806	2.885	2.283	2.025	0.898
50	HSDBT	4.901	3.808	2.902	2.301	2.044	0.903
	ASDBT	4.901	3.811	2.902	2.301	2.044	0.903
100	CBT	4.906	3.812	2.905	2.305	2.047	0.904
	HSDBT	4.905	3.811	2.904	2.304	2.047	0.904
	ASDBT	4.905	3.812	2.904	2.304	2.047	0.904

*Full ceramic; **Full metal

$$w(x) = a\sin\pi\frac{x}{L} \tag{31}$$

$$u_1(x) = b\cos\pi\frac{x}{L} \tag{32}$$

Where, the two unknowns a and b remain to be determined. By replacing the values of the equations of the simply supported boundary conditions (31) and (32) in the relation established by Eqs. (25) and (26), three solutions of this problem are obtained: the first trivial solution $a = 0$ presents an equilibrium position formulation in the prebuckling state, two other solutions $a \neq 0$ must be additionally verified at stable equilibrium positions in the postbuckling state. The postbuckling response according to the principle beyond the buckling state at the prebuckling equilibrium position becomes unstable as follows

$$a = \pm\frac{2}{\pi\sqrt{A_{11}}}\sqrt{\bar{N}L^2 - \pi^2 D_{11} + \frac{\pi^4 F_{11}^2}{L^2 A_{55} + \pi^2 H_{11}}} \tag{33}$$

For the condition at midspan of the beam where *x*=*L*/2 we obtain the buckling load amplitude a corresponds to the maximum buckling level.

By using the linear counterpart of Eq. (25), the resolve can be expressed the critical buckling $\bar{N}_{cr}$ load as follows

$$\bar{N}_{cr} = \frac{\pi^2}{L^2}\left(D_{11} - \frac{\pi^2 F_{11}^2}{L^2 A_{55} + \pi^2 H_{11}}\right) \tag{34}$$

3. Results and discussion

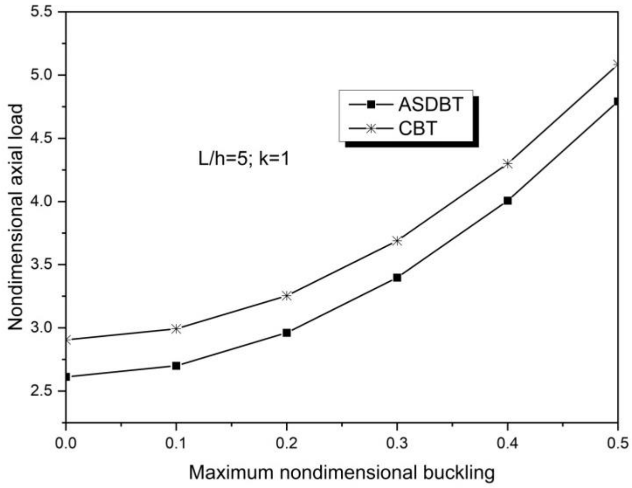

Fig. 3 Variation of the maximum buckling with the applied axial load for *L/h*=5 and *k*=1

In numerical analysis, critical buckling loads of FG beams with simply supports are given in tabular form for different values of slenderness ratio (*L/h*). The FGM beams are made of aluminum (Al; $E_m = 70GPa$; $\nu_m = 0.3$) and alumina ($Al_2\ O_3$; $E_c = 380GPa$; $\nu_c = 0.3$) and their properties change through the thickness of the beam according to power-law. In the present study, the top surfaces of the FG beams are alumina rich, whereas the bottom surfaces of the FG beams are aluminum rich. In addition, the critical buckling loads are non-dimensionalized by

$$\bar{N}_{cr} = \frac{\pi^2}{L^2}\left(D_{11} - \frac{\pi^2 F_{11}^2}{L^2 A_{55} + \pi^2 H_{11}}\right) \tag{35}$$

Firstly, Table 1 shows the variation results of the non-dimensional first critical buckling load of simply supported beams for different values of material parameters and different values of length-to-thickness ratios *L/h*=5, 10, 20, 50 and 100, respectively. We note that decreasing the value of the power-law exponent will lead to an increase in the critical buckling load. The lowest critical buckling load values are obtained for full metal beam (*k*→∞) while the highest critical buckling load values are obtained for full ceramic beam (*k*=0). This is due to the fact that as seen from Fig. 2, an increase in the value of the power-law exponent results in a decrease in the value of elasticity modulus and the value of bending rigidity. In other words, the beam becomes flexible as the power law exponent increases.

Figs. 3 and 4 present the variation of the critical buckling load of a simply supported FG beam with the dimensionless amplitude for two values of the slenderness ratio *L/h* (*L/h*=5 and 10, respectively), with material parameter (*k*=1) using the two theories CBT and ASDBT. From these two figures it is clearly observed that the increase of dimensionless amplitude causes the increase of dimensionless axial load monotonically. It can also be seen that the critical buckling load increases when the slenderness ratio (*L/h*) increases. On the other hand, the values of the dimensionless axial load obtained by using the ASDBT theory are lower than those obtained by using the CBT theory, this is due to the transverse shear effect.

Fig. 5 gives the variation the variation of the nondimensional axial load of FGM beam with *L/h* ratio for different values of volume fraction exponent *k* by using the two theories of beams CBT

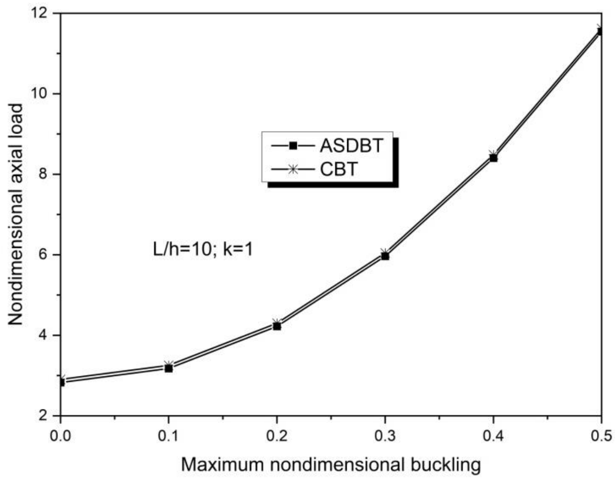

Fig. 4 Variation of the maximum buckling with the applied axial load for *L/h*=10 and *k*=1

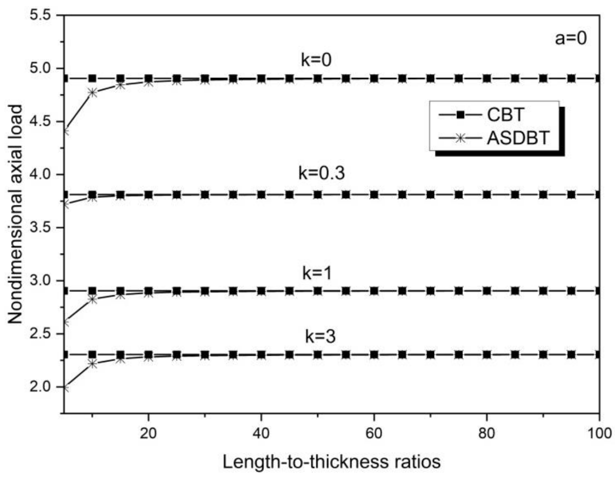

Fig. 5 Variation of the maximum buckling of simply supported FGM beam with *L/h* ratio for various values of the power-law exponent with *a*=0

and ASDBT. This figure can be considered as the visual representation of part of Table 1. As shown in this figure, there is a remarkable difference between the non-dimensional axial load of CBT and those of shear deformable beam theory when the slenderness ratio of FGM beam is less than *L/h*=20. This means that for short beams (i.e., *L/h*.10), in particular, shear deformable beam theories should be used in the analysis. Also, critical buckling load of the FGM beam is saturated after the value of (*L/h*=20). Also, note that the power-law exponent plays an important role on the critical buckling load of the FGM beam.

4. Conclusions

In this work, an analytical method for post-buckling analysis of functionally graded beams has been employed to study the critical buckling load and static post-buckling response of FG beams with simply supported boundary conditions based on classical theory, and two higher order shear deformation theories. Furthermore, parametric studies of the effects of material variations and slenderness ratio are examined and presented in detail. The following conclusions can be drawn from the analysis results of FG beams:

- The spatial and progressive variation of the properties of functionally graded materials allows the creation of innovative structures that can be exploited in many fields of application in special structures in engineering.
- When the slenderness ratio L/h increases, the values of the nondimensional critical buckling load will increase.
- Remarkable differences can be seen between the dimensionless critical buckling load of higher-order beam theory and those of classical beam theory when $L/h < 20$.
- Negligible differences can be observed for long FGM beams, i.e., $L/h \geq 20$; between the dimensionless critical buckling load of higher order beam theory and those of CBT.
- The increase in the value of the parameter of the power law exponent causes a decrease in the values of the non-dimensional critical buckling load;
- The two higher order beam theories give very close results.

Finally, it can be said that this modest work contributed in the understanding of the behavior of composite beams with functional graded and the tabulated results will serve as a reference with which other researchers can compare their approaches.

References

Amara, K., Bouazza, M. and Fouad, B. (2016), "Postbuckling analysis of functionally graded beams using nonlinear model", *Per. Polytech. Mech. Eng.*, **60**(2), 121-128. https://doi.org/10.3311/ppme.8854.

Arefi, M. (2015), "Elastic solution of a curved beam made of functionally graded materials with different cross sections", *Steel Compos. Struct.*, **18**(3), 659-672. https://doi.org/10.12989/scs.2015.18.3.659.

Arefi, M. and Najafitabar, F. (2021), "Buckling and free vibration analyses of a sandwich beam made of a soft core with FG-GNPs reinforced composite face-sheets using Ritz Method", *Thin. Wall. Struct.*, **158**, 107200. https://doi.org/10.1016/j.tws.2020.107200.

Arefi, M. and Soltan Arani, A.H. (2018), "Higher order shear deformation bending results of a magnetoelectrothermoelastic functionally graded nanobeam in thermal, mechanical, electrical, and magnetic environments", *Mech. Bas. Des. Struct.*, **46**(6), 669-692. https://doi.org/10.1080/15397734.2018.1434002.

Arefi, M. and Zenkour, A.M (2017c), "Size-dependent vibration and bending analyses of the piezomagnetic three-layer nanobeams", *Appl. Phys. A*, **123**, 202. https://doi.org/10.1007/s00339-017-0801-0.

Arefi, M. and Zenkour, A.M. (2016), "A simplified shear and normal deformations nonlocal theory for bending of functionally graded piezomagnetic sandwich nanobeams in magneto-thermo-electric environment", *J. Sandw. Struct. Mater.*, **18**(5), 624-651. https://doi.org/10.1177/1099636216652581.

Arefi, M. and Zenkour, A.M. (2017a), "Wave propagation analysis of a functionally graded magneto-electro-elastic nanobeam rest on Visco-Pasternak foundation", *Mech. Res. Commun.*, **79**, 51-62. https://doi.org/10.1016/j.mechrescom.2017.01.004.

Arefi, M. and Zenkour, A.M. (2017b), "Vibration and bending analysis of a sandwich microbeam with two integrated piezomagnetic face-sheets", *Compos. Struct.*, **159**, 479-490. https://doi.org/10.1080/01495739.2016.1229146.

Arefi, M. and Zenkour, A.M. (2017d), "Transient sinusoidal shear deformation formulation of a size-dependent three-layer piezo-magnetic curved nanobeam", *Acta Mechanica*, **228**, 3657-3674.

https://doi.org/10.1007/s00707-017-1892-6.
Arefi, M. and Zenkour, A.M. (2017e), "Transient analysis of a three-layer microbeam subjected to electric potential", *Int. J. Smart Nano Mater*., **8**(1), 20-40. https://doi.org/10.1080/19475411.2017.1292967.
Arefi, M. and Zenkour, A.M. (2018), "Size-dependent electroelastic analysis of a sandwich microbeam based on higher-order sinusoidal shear deformation theory and strain gradient theory", *J. Intel. Mater. Syst. Struct*., **29**(7), 1394-1406. https://doi.org/10.1177/1045389X17733333.
Arefi, M. and Zenkour, A.M. (2019), "Influence of magneto-electric environments on size-dependent bending results of three-layer piezomagnetic curved nanobeam based on sinusoidal shear deformation theory", *J. Sandw. Struct. Mater*., **21**(8), 2751-2778. https://doi.org/10.1177/1099636217723186.
Arefi, M., Mohammad-Rezaei Bidgoli, E., Dimitri, R., Bacciocchi, M. and Tornabene, F. (2019), "Nonlocal bending analysis of curved nanobeams reinforced by graphene nanoplatelets", *Compos. Part B Eng*., **166**, 1-12. https://doi.org/10.1016/j.compositesb.2018.11.092.
Atmane, H.A., Bedia, E.A.A., Bouazza, M., Tounsi, A. and Fekrar, A. (2016), "On the thermal buckling of simply supported rectangular plates made of a sigmoid functionally graded Al/Al2O3 based material", *Mech. Solid*., **51**, 177-187. https://doi.org/10.3103/S0025654416020059.
Becheri, T., Amara, K., Bouazza, M. and Benseddiq, N. (2016), "Buckling of symmetrically laminated plates using nth-order shear deformation theory with curvature effects", *Steel Compos. Struct*., **21**(6), 1347-1368. https://doi.org/10.12989/scs.2016.21.6.1347.
Bouazza, M. and Adda-Bedia, E.A. (2013), "Elastic stability of functionally graded rectangular plates under mechanical and thermal loadings", *Sci. Res. Essays*, **8**(39), 1933-1943. https://doi.org/10.5897/SRE11.251.
Bouazza, M. and Zenkour, A.M. (2021), "Vibration of inhomogeneous fibrous laminated plates using an efficient and simple polynomial refined theory", *J. Comput. Appl. Mech*., **52**, 233-245. https://doi.org/10.22059/jcamech.2021.320751.605.
Bouazza, M., Antar, K., Amara, K., Benyoucef, S. and Bedia, E. (2019a), "Influence of temperature on the beams behavior strengthened by bonded composite plates", *Geomech. Eng*., **18**(5), 555-566. https://doi.org/10.12989/gae.2019.18.5.555.
Bouazza, M., Becheri, T., Boucheta, A. and Benseddiq, N. (2019b), "Bending behavior of laminated composite plates using the refined four-variable theory and the finite element method", *Earthq. Struct*., **17**(3), 257-270. https://doi.org/10.12989/eas.2019.17.3.257.
Bouazza, M., Zenkour, A.M. and Benseddiq, N. (2017), "Effect of material composition on bending analysis of FG plates via a two-variable refined hyperbolic theory", *Arch. Mech*., **70**(2), 107-129.
Boucheta, A., Bouazza, M., Becheri, T., Eltaher, M.A., Tounsi, A. and Benseddiq, N. (2024), "Bending of sandwich FGM plates with a homogeneous core either hard or soft via a refined hyperbolic shear deformation plate theory", *Iran. J. Sci. Technol. Trans. Ciilv Eng*., 1-15. https://doi.org/10.1007/s40996-024-01386-w.
Chakraborty, A. and Gopalakrishnan, S.A. (2003), "Spectrally formulated finite element for wave propagation analysis in functionally graded beams", *Int. J. Solid. Struct*., **40**, 2421-2448. https://doi.org/10.1016/S0020-7683(03)00029-5.
Chaudhari, V.K., Shegokar, N.L. and Lal, A. (2017), "Stochastic thermo-mechanically induced post buckling response of elastically supported nanotube-reinforced composite beam", *Adv. Aircraft Spacecraft Sci*., **4**(5), 585-611. https://doi.org/10.12989/aas.2017.4.5.585 585.
Derbale, A., Bouazza, M. and Benseddiq, N. (2021), "Analysis of the Mechanical and Thermal Buckling of Laminated Beams by New Refined Shear Deformation Theory", *Iran. J. Sci. Technol. Tran. Civil Eng*., **45**, 89-98. https://doi.org/10.1007/s40996-020-00417-6.
Ebrahimi, F. and Farazmandnia, N (2018), "Vibration analysis of functionally graded carbon nanotube reinforced composite sandwich beams in thermal environment", *Adv. Aircraft Spacecraft Sci*., **5**(1), 107-128. https://doi.org/10.12989/aas.2018.5.1.107.
Ellali, M., Alazwari, M.A., Bouazza, M., Eltaher, M.A. and Benseddiq, N. (2024e), "Effects of changing materials properties for vibration of FGM beam using integral shear deformation model", *Couple. Syst. Mech*., **13**(4), 277-291. https://doi.org/10.12989/csm.2024.13.4.27.7.

Ellali, M., Amara, K. and Bouazza, M. (2024c), "Thermal buckling of porous FGM plate integrated surface-bonded piezoelectric", *Couple. Syst. Mech.*, **13**(2), 171-186. https://doi.org/10.12989/csm.2024.13.2.171.

Ellali, M., Amara, K., Bouazza, M. and Bourada, F. (2018), "The buckling of piezoelectric plates on pasternak elastic foundation using higher-order shear deformation plate theories", *Smart Struct. Syst.*, **21**(1), 113-122. https://doi.org/10.12989/SSS.2018.21.1.113.

Ellali, M., Bouazza, M. and Amara, K. (2022), "Thermal buckling of a sandwich beam attached with piezoelectric layers via the shear deformation theory", *Arch. Appl. Mech.*, **92**, 657-665. https://doi.org/10.1007/s00419-021-02094-x.

Ellali, M., Bouazza, M. and Zenkour, A.M (2023), "Wave propagation of FGM plate via new integral inverse cotangential shear model with temperature-dependent material properties", *Geomech. Eng.*, **33**(5), 427-437. https://doi.org/10.12989/gae.2023.33.5.427.

Ellali, M., Bouazza, M. and Zenkour, A.M. (2024a), "Hygrothermal vibration of FG nanobeam via nonlocal unknown integral variables secant-tangential shear deformation coupled theory with temperature-dependent material properties", *Eur. J. Mech. A/Solid.*, **10**5, 105243. https://doi.org/10.1016/j.euromechsol.2024.105243.

Ellali, M., Bouazza, M., Zenkour, A.M. and Benseddiq, N. (2024b), "Polynomial-exponential integral shear deformable theory for static stability and dynamic behaviors of FG-CNT nanobeams", *Arch. Appl. Mech.*, 1-20. https://doi.org/10.1007/s00419-024-02582-w.

Ellali, M., Zenkour, A.M., Bouazza, M. and Benseddiq, N, (2024d)., "Thermal buckling of FG nanobeams via an indeterminate integral variable with trigonometric displacement models in conjunction with the gradient elasticity theory", *J. Nano Res.*, **82**, 117-138. https://doi.org/10.4028/p-PCOnh6.

Ghasemi, A.R. and Masood Mohandes, M. (2016), "The effect of finite strain on the nonlinear free vibration of a unidirectional composite Timoshenko beam using GDQM", *Adv. Aircraft Spacecraft Sci.*, **3**(4), 379-397. https://doi.org/10.12989/aas.2016.3.4.379.

Hosseini, S.A.H., Moghaddam, M.H.N. and Rahmani, O. (2020), "Exact solution for axial vibration of the power, exponential and sigmoid FG nonlocal nanobeam", *Adv. Aircraft Spacecraft Sci.*, **7**(6), 517-536. https://doi.org/10.12989/aas.2020.7.6.517.

Houari, M.S.A., Bessaim, A., Merzouki, T., Daikh, A.A., Garg, A., Tounsi, A. and Belarbi, M.O. (2024), "Shear correction factors of a new exponential functionally graded porous beams", *Struct. Eng. Mech.*, **89**(1), 1-11. https://doi.org/10.12989/sem.2024.89.1.001.

Karama, M., Afaq, K.S. and Mistou, S. (2003), "Mechanical behavior of laminated composite beam by new multi-layered laminated composite structures model with transverse shear stress continuity", *Int. J. Solid. Struct.*, **40**, 1525-1546. https://doi.org/10.1016/S0020-7683(02)00647-9.

Kenouza, Y., Bouazza, M., Zenkour, A.M. and Benseddiq, N. (2024), "Vibrations analysis of antisymmetric/symmetric laminated composite plates via refined simplified nth-higher-order shear deformation theory", *Earthq. Struct.*, **27**(6), 445-456. https://doi.org/10.12989/eas.2024.27.6.445.

Nayfeh, A.H. and Emam, S.A (2008), "Exact solution and stability of postbuckling configurations of beams", *Nonlin. Dyn.*, **54**(4), 395-408. https://doi.org/10.1007/s11071-008-9338-2.

Nguyen, D.K. and Tran, T.T. (2018), "Free vibration of tapered BFGM beams using an efficient shear deformable finite element model", *Steel Compos. Struct.*, **29**(3), 363-377. https://doi.org/10.12989/scs.2018.29.3.363.

Osman, T., Mohamed, S.A., Eltaher, M.A., Alazwari, M.A. and Mohamed, N. (2024), "Vibration of bio-inspired laminated composite beams under varying axial loads", *Steel Compos. Struct.*, **50**(1), 25-43. https://doi.org/10.12989/scs.2024.50.1.025.

Qing, H. and Cai, Y. (2023), "Semi-analytical and numerical post-buckling analysis of nanobeam using two-phase nonlocal integral models", *Arch. Appl. Mech.*, **93**, 129-149. https://doi.org/10.1007/s00419-021-02099-6.

Sankar, B.V. (2001), "An elasticity solution for functionally graded beams", *Compos. Sci. Technol.*, **61**, 689-96.

Selmi, A. (2020), "Dynamic behavior of axially functionally graded simply supported beams", *Smart Struct. Syst.*, **25**(6), 669-678. https://doi.org/10.12989/sss.2020.25.6.669.

Simsek, M. and Kocaturk, T. (2009), "Free and forced vibration of a functionally graded beam subjected to a concentrated moving harmonic load", *Compos. Struct.*, **90**(4), 465-473. https://doi.org/10.1016/j.compstruct.2009.04.024.

Soldatos, K.P. and Timarci, T. (1993), "A unified formulation of laminated composites, shear deformable, five-degrees-of-freedom cylindrical shell theories", *Compos. Struct.*, **25**, 165-171. https://doi.org/10.1016/0263-8223(93)90162-J.

Tang, Y. and Qing, H. (2023), "Size-dependent nonlinear post-buckling analysis of functionally graded porous Timoshenko microbeam with nonlocal integral models", *Commun. Nonlin. Sci.*, **116**, 106808. https://doi.org/10.1016/j.cnsns.2022.106808.

Tounsi, A., Bouazza, M. and Adda-Bedia, E. (2004), "Computation of transient hygroscopic stresses in unidirectional laminated composite plates with cyclic and asymmetrical environmental conditions", *Int. J. Mech. Mater. Des.*, **1**, 271-286. https://doi.org/10.1007/s10999-005-0222-7.

Tounsi, A., Bouazza, M., Meftah, S. and Adda-Bedia, E. (2005), "On the transient hygroscopic stresses in polymer matrix laminated composites plates with cyclic and unsymmetric environmental conditions the moisture concentration", *Polym. Polym. Compos.*, **13**(5), 489-503. https://doi.org/10.1177/096739110501300506.

Wang, Q. and Yu, W. (2014), "A variational asymptotic approach for thermoelastic analysis of composite beams", *Adv. Aircraft Spacecraft Sci.*, **1**(1), 93-123. http://doi.org/10.12989/aas.2014.1.1.093.

Xu, Y., Li, Z. and Guo, K. (2018), "Active vibration robust control for FGM beams with piezoelectric layers", *Struct. Eng. Mech.*, **67**(1), 33-43. https://doi.org/10.12989/SEM.2018.67.1.033.

Yang, J. and Chen, Y. (2008), "Free vibration and buckling analyses of functionally graded beams with edge cracks", *Compos. Struct.*, **83**(1), 48-60. https://doi.org/10.1016/j.compstruct.2007.03.006.

Zhong, Z. and Yu, T. (2007), "Analytical solution of a cantilever functionally graded beam", *Compos. Sci. Technol.*, **67**, 481-488. https://doi.org/10.1016/j.compscitech.2006.08.023.

CC